Improved design for large wind turbine blades of fibre composites (Phase 4) - Summary report

Sørensen, Bent F.; Toftegaard, Helmuth Langmaack; Goutianos, Stergios; Branner, Kim; Berring, Peter; Lund, E.; Wedel-Heinen, J.; Garm, J.H.

Publication date:
2010

Document Version
Publisher's PDF, also known as Version of record

Improved design for large wind turbine blades of fibre composites (Phase 4) - Summary report

Risø-R-Report

B. F. Sørensen, H. Toftegaard, S. Goutianos, K. Branner, P. Berring, E. Lund, J. Wedel-Heinen and J. H. Garm
Risø-R-1734(EN)
June 2010

Risø DTU
National Laboratory for Sustainable Energy

Author: B. F. Sørensen[1], H. Toftegaard[1], S. Goutianos[1], K. Branner[2], P. Berring[2], E. Lund[3], J. Wedel-Heinen[4] and J. H. Garm[5]
Title: Improved design for large wind turbine blades of fibre composites (Phase 4) - Summary report
Division: [1]Materials Research Division, Risø DTU, [2]Wind Energy Division, Risø DTU, [3]Department of Mechanical Engineering, Aalborg University, [4]Vestas Wind System, [5]LM Wind Power

Risø-R-1734(EN)
June 2010

ISSN 0106-2840
ISBN 978-87-550-3825-7

Abstract (max. 2000 char.):

Results are summarised for the project "Improved design for large wind turbine blades (Phase 4)", partially supported by the Danish Energy Agency under the Ministry of Climate and Energy through the EUDP journal no.: 33033-0267. The aim of the project was to develop new and better design methods for wind turbine blades, so that uncertainties associated with damage and defects can be reduced. The topics that are studied include buckling-driven delamination of flat load-carrying laminates, cracking along interfaces in material joints (fracture mechanical characterisation and modelling), cyclic crack growth with large scale bridging and the use of cohesive laws in finite element programmes for simulating wind turbine blade failure. An overview is given of the methods and the major research results of the project. The implementation of the knowledge in the industry is discussed. Finally, some ideas for future research activities are considered.

Group's own reg. no.:
1615116-00

Sponsorship:
The Danish Energy Agency under the Ministy of Climate and Energy

Pages: 38
Tables: 1
References: 45

Information Service Department
Risø National Laboratory for Sustainable Energy
Technical University of Denmark
P.O.Box 49
DK-4000 Roskilde
Denmark
Telephone +45 46774005
bibl@risoe.dtu.dk
Fax +45 46774013
www.risoe.dtu.dk

Contents

Preface

This summary-report contains an overview of the activities of the project "Improved design for large wind turbine blades (Phase 4)", partially supported by the Danish Energy Agency under the Ministry of Climate and Energy through the EFP-grant no. 33033-0267. The project ran from 2008 to 2009. The project participants were: The Materials Research Division, Risø DTU (project leader), The Wind Energy Division, Risø DTU, The Department of Mechanical Engineering, Aalborg University, LM Wind Power A/S and Vestas Wind Systems A/S. The project was a continuation of the project "Improved design for large wind turbine blades, based on studies of scale-effects (Phase 1)" (J. no. 1363/01-01-0007), the project "Improved design for large wind turbine blades, based on studies of scale-effects (Phase 2)" (J. no. 1363/03-0006) and "Improved design for large wind turbine blades (Phase 3)", partially supported by the Danish Energy Agency under the Ministry of Climate and Energy through the (J. no 33031-0078).

1 Introduction

1.1 Background

Wind energy is a sustainable energy source that provides a significant amount of the Danish electricity production. It is expected that the amount of electricity produced by wind turbines will increase in the coming year as more wind turbines are being installed. In Denmark, as probably in most North Europe, a major part of the increase in wind energy will come from large wind turbines placed off-shore in big wind farm parks.

The rotor blades are the largest rotating components of a wind turbine. They are made of light and strong, fatigue resistant composite materials (e.g. glass fibre and carbon fibre composites), low-weight core materials (such as balsa wood or polymer foam), often bonded together by polymer adhesives. Various types of damage, cracks and failure modes, such as (buckling-driven) delamination and failure of adhesive joints can develop in wind turbine rotor blades (Sørensen et al., 2004). Often, damage develops from manufacturing-induced flaws. The initiation process is difficult to model, however, once well-defined cracks have formed, *fracture mechanics* methods are applicable. In order to be able to model and thus understand the evolution of damage in a wind turbine blade, the relevant fracture mechanics properties of each material and the interfaces between the materials must be characterised.

The focus area of this project is thus the *damage evolution and failure of large wind turbine blades* made of composite materials. The main aim is to develop new and better experimental and modelling methods for failure modes encountered in wind turbine blades. The long term aim is to develop reliable simulation tools (the "virtual blade") that allows quantitative predictions of the strength and fatigue lifetime of wind turbine blade with damages, based on knowledge of the damage/crack types, size and location in the wind turbine blade as well as the appropriate fracture mechanics properties. The tools that we aim to develop are *general methods* and will be demonstrated for *generic problems* (i.e., not optimisation of specific design details).

The two major development trends in wind energy

- larger size wind turbines
- off-shore placement

lead to major challenges.

Concerning the *increase in size* of blades, it is important to note that wind turbine blades are made of relative few, but large parts. Since a large blade part (made of composite materials) has a large value (due to its size, much material is used for each part), it is unattractive to discard it. Only blades with manufacturing defects that will initiate damage and cracks should be repaired or discarded. Thus, it is of great importance possess technology in the form of knowledge of how to detect manufacturing defects and how to predict evolution of damage and crack growth and potentially blade failure during service.

Concerning *off-shore placement*, it is obvious that access to off-shore wind turbines is more difficult and costly than for land-based wind turbines. It is thus necessary to reduce the need for manual inspection as much as possible. Potentially, this can be done by the use of build-in sensors for *structural health monitoring*. However, several challenges remain: First, sensors need to be demonstrated (i.e., the relationship between damage

type, damage size and location and sensor signals should be proven). Secondly, having successfully identified the type, size and location of some damage by sensors, next step is to evaluate the identified damage: Is it serious? Should the blade be repaired? How large can the damage be allowed to grow before it reduces the load-carrying capability of the blade critically? Such questions can only be answered if computational tools are available that allows the modelling of the specific type, size and location of the damage and the appropriate fracture mechanics properties of the materials (and interface between dissimilar materials) are known. Thirdly, well-documented repair procedures for wind turbine blades should be available.

Some of the required knowledge and tools are not yet available. The present project, however, aims for establishing general tool for addressing some of the required issues.

We aim for establishing and verifying design tools that are based on fracture mechanics. As described in the Phase 3 Summary report (Sørensen et al., 2009), the scientific aims are to develop *general tools* for various failure modes by the following approach:

1. developing *new fracture mechanics characterisation methods* for the measurement of relevant fracture mechanics parameters
2. developing *new modelling tools* for predicting the load-carrying capabilities of structures
3. experimental *verification* of the characterisation methods and modelling tools by case studies using generic specimens

It should be noted that the commonly used probabilistic design approach, where uncertainties are described in terms of statistical functions, cannot be used in the same manner in the decision-making of blades with detected damages. Thus, the use of fracture mechanics induces a *paradigm shift* in the approach to strength prediction of wind turbine blade structures.

1.2 Purpose

The overall, long-term goal of this project (Phase 1 to Phase 4) is to develop general characterisation and modelling tools for failure modes encountered in large wind turbine blades, so that the mechanical properties of the materials can be fully utilised and the structural design can be optimised. The new design methods enable the wind turbine industry to improve their design details and their choice of materials and thus impart a higher level of safety/quality of their products.

The specific problems investigated in this project (Phase 4) are largely a continuation of problems studied in Phase 3: Failure of materials joints experiencing large-scale bridging (cracking along the interface between dissimilar materials), failure of composite panels subjected to compressive loads (buckling-driven delamination) and modelling of damage in a global model of a wind turbine blade. A new topic introduced in Phase 4 is: Cyclic crack growth in composite materials experiencing large-scale bridging.

Being a summary report, this report only contains a brief collection of the research topics and the major results. For more details, see the publications listed in the end of this report.

2 Buckling and compressive strength

2.1 Introduction

Delaminations are considered one of the most critical types of damage that can occur in laminated structures (Abrate, 1991). They can be defined as areas with no bonding between adjacent layers and usually originate from either manufacturing flaws or from impact damage during production, transport or service.

In wind turbine blades, the flapwise bending loads are typically carried by thick, solid and slightly curved composite panels extending in the whole length of the blade. These load carrying thick laminates are the flanges in the main spar of the blade (see Figure 2.1) and experience compressive loading when the blade is bending towards that side. It may therefore be critical when delaminations occur in these load carrying laminates.

A panel with a delamination, subjected to compressive loading may buckle and fail in two different ways. The panel may buckle in a *local buckling mode*, where the sub-laminate on one side of the delamination buckles, which typically occurs when the delamination is large in size and positioned close to one of the surfaces. The other buckling mode is *global bucking* where both the sub-laminate and the remaining panel buckle toward the same side of the panel, which typically occurs when the delamination is small and deep in the laminate. In the local buckling mode, the buckling may drive a growth of the delamination leading to panel failure (buckling-driven delamination).

The aim of this study is to investigate how much the compressive strength of flat and slightly curved composite panels is reduced due to a delamination and to study which conditions leads to growth of the delamination.

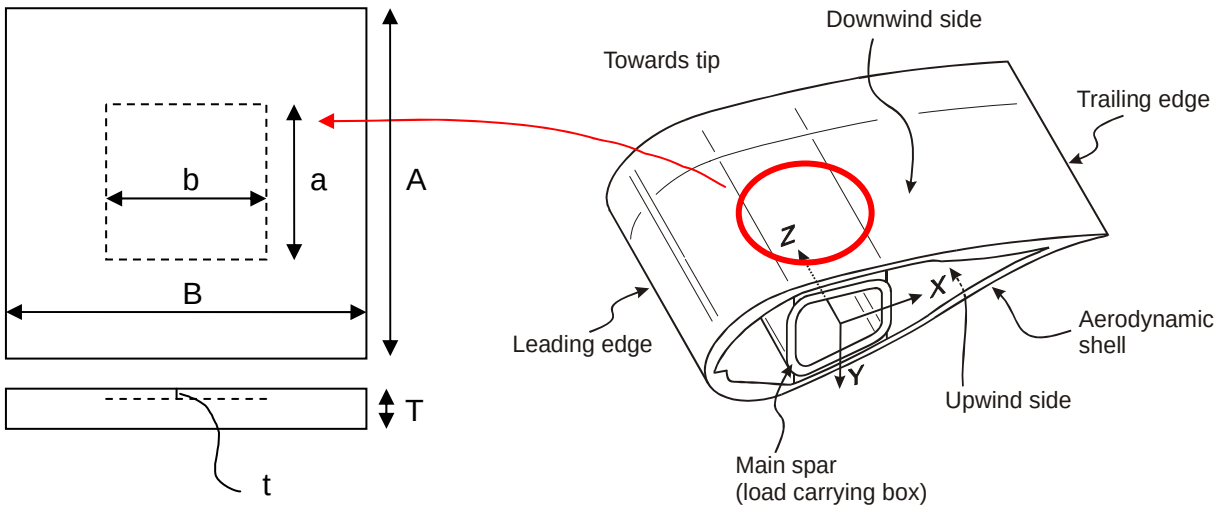

Figure 2.1 Description of test specimens, which are similar to the load carrying laminate in the main spar of a typical wind turbine blade.

2.2 Experimental work

During this phase and the previous phase of the project, a large number of flat composite panels with and without delaminations have been tested until failure. The test specimens are rectangular composite panels made of glass fibre reinforcement plastic. The lay-up is symmetric with approximately 90% of the reinforcement in the load direction and the remaining reinforcement in the ±45º directions. Two different types of panels were tested. One type was made with prepregs and the other type was made using the vacuum infusion technique. Even though the specimens were made similar to the load carrying laminate in a typical wind turbine blade, the material properties are not representative to those in real wind turbine blades, as the specimens were produced in the lab under different conditions.

For both types, some of the panels were manufactured with no intentional defects or imperfections, while others had Teflon sheets embedded to simulate delaminated rectangular areas of different size (*a/A* & *b/B*) and depth (*t/T*) as shown in Figure 2.1. A specially designed test rig (see Sørensen et al. 2009) was used in a 5 MN Instron testing machine. The rig is designed to limit rotation and out-of-plane deflection of the edges of the panels. The panels were loaded to ultimate failure and a digital image correlation (DIC) measurement system was used in addition to conventional displacement transducers to monitor full field displacements of the panels under increasing load.

2.2.1 Robust method to determine buckling load

In the previous phase of the project, a method was developed in order to determine the buckling load (Sørensen et al. 2009). However, it has turned out that this method is too sensitive to scatter in the experimental data. In order to ensure consistency for all delaminations sizes and through thickness positions, a robust method for estimating the buckling load was applied in both the experimental and numerical studies. The normalized in-plan force was plotted vs. the normalized in-plan displacement. In the start of the load history, the response of the panels is linear, but as the panels start to buckle, the response becomes nonlinear.

A linear curve is determined by the first 30% of this load history and then offset by 2.5%. The buckling load is then found as the load at the intersection between this linear curve and a spline interpolation of the entire load history, see Figure 2.2.

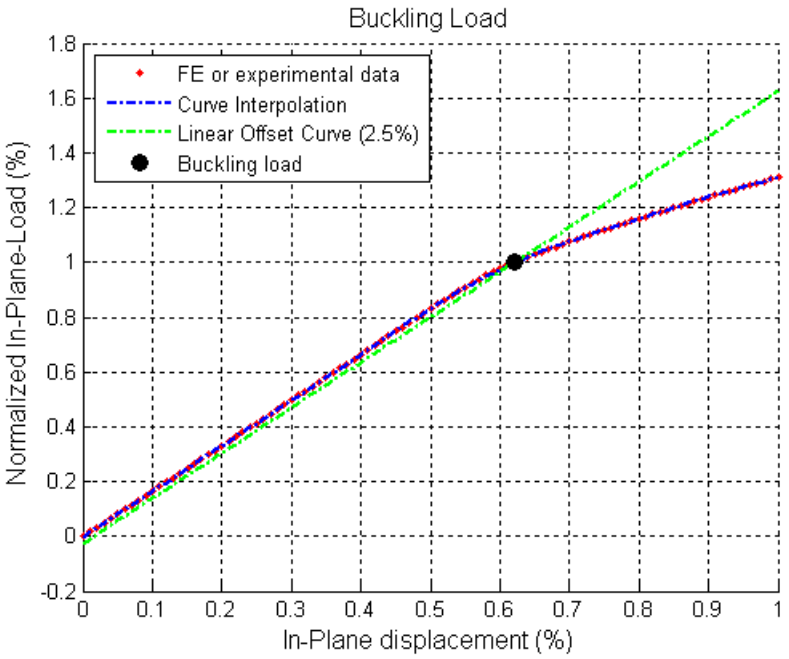

Figure 2.2 Robust method to determine buckling load.

2.2.2 Test results

Table 1 lists the main results from the experimental panel tests. The panels have delaminations of different size and through thickness position. For a few of the panels, strange behavior was observed or measuring equipment was not running properly. These panels are not included here. In Table 1, average results are shown for between 2 and 4 specimens of each type.

The buckling load was determined for each panel using the method described in the previous section. The average buckling loads for the small series of each type is denoted P_i and the average buckling loads for panels without delaminations is denoted P_n. The two different panel types with respect to manufacturing process were treated separately meaning that they have different P_n.

Table 1 List of the tested specimens with delamination size and through thickness position for the two different production types (A & B). The observed buckling mode is listed together with the measured reduced strength, calculated as the average buckling load for that delamination (P_i) relatively to the average buckling load for that type of panel without delamination (P_n).

Test panels					**Failure**	
Code	Specimens	a/A	b/B	t/T	Type	P_i/P_n
A4	2		None		Global	100%
A5a	3	0,48	0,39	0,31	Global	81%
A5b	4	0,47	0,39	0,21	Local	87%
A6a	2	0,36	0,30	0,31	Global	87%
A6b	4	0,35	0,30	0,21	Local	83%
A7a	2	0,42	0,34	0,25	Global	92%
A7b	4	0,41	0,34	0,16	Local	82%
B5	3		None		Global	100%
B6	3	0,82	0,64	0,29	Local	54%
B7	3	0,63	0,49	0,29	Local?	63%
B8	2	0,68	0,54	0,25	Local?	57%

2.3 Numerical parameter study

Numerical parameter studies have been conducted on both flat and slightly curved panels.

2.3.1 FE-models

The finite-element models were modeled with 20-node orthotropic solid elements. Two or three elements were used through the thickness depending on the through thickness position of the delamination.

A small out-of-plane displacement corresponding to the first buckling mode shape was applied as an initial imperfection of the delaminated sub-laminate. The amplitude of the initial imperfections was approximately 0.5‰ of the panel thickness for the flat panels and approximately 0.5% of the panel thickness for the curved panels.

The elements were all joined in the interfaces, except for the delaminated area where quadratic contact conditions were applied to prevent penetration. The average number of degrees of freedom (DOFs) was approximately 150.000.

Nonlinear geometric analyses were conducted with minimum 100 increments to ensure that a well described and smooth graph could be made for in-plane force vs. out-of-plane displacement. Typical models and behavior is shown in Figure 2.3.

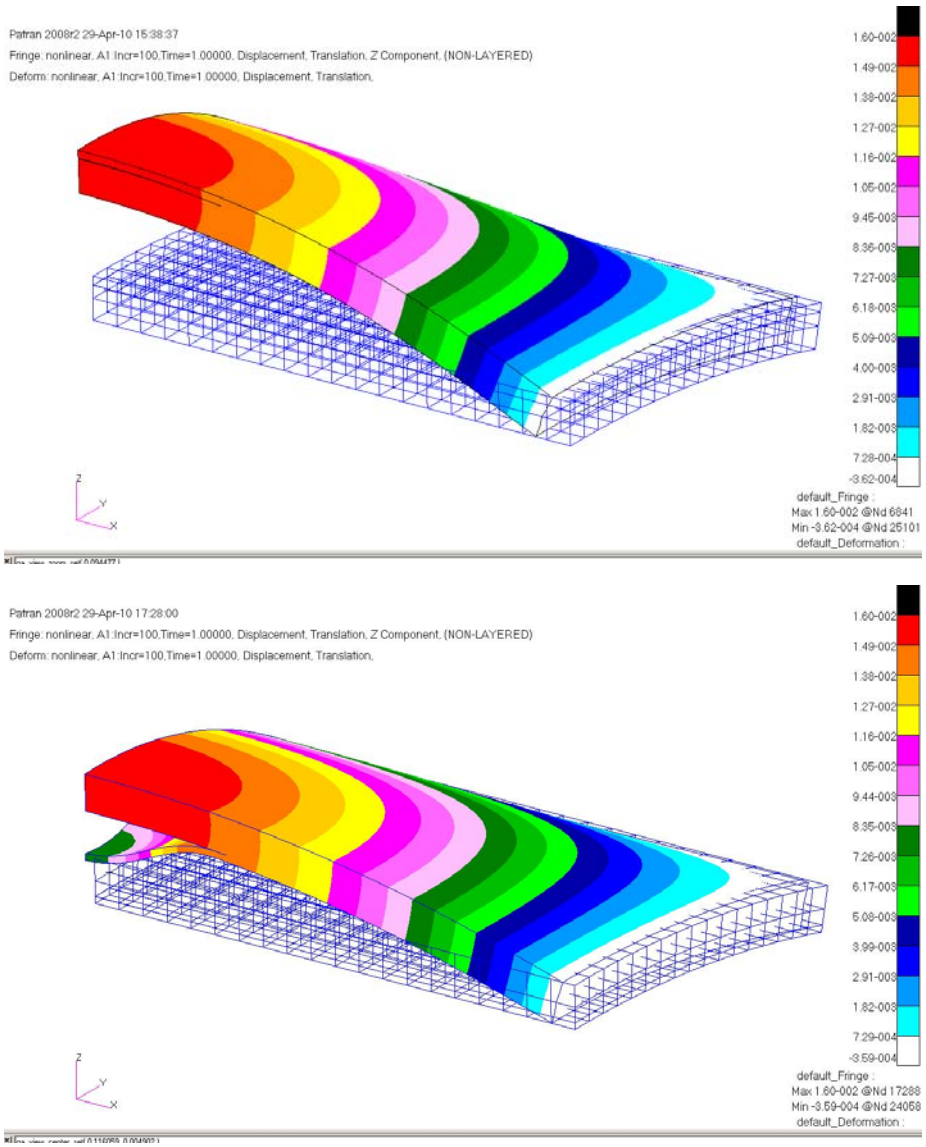

Figure 2.3 Typical finite element results (one quarter of model) for curved panels showing global buckling (top) and local buckling (bottom) modes respectively. Colors indicate the magnitude of the out-of-plane displacements.

2.3.2 Compressive strength of flat panels

The reduced compressive strength due to delaminations for flat panels was treated in the previous phase of the project (Sørensen et al. 2009). However, a new and more robust method to determine the buckling load was introduced in this phase of the project as described earlier. Based on the nonlinear numerical analyses new strength reduction maps were produced for flat panels as shown in Figure 2.4.

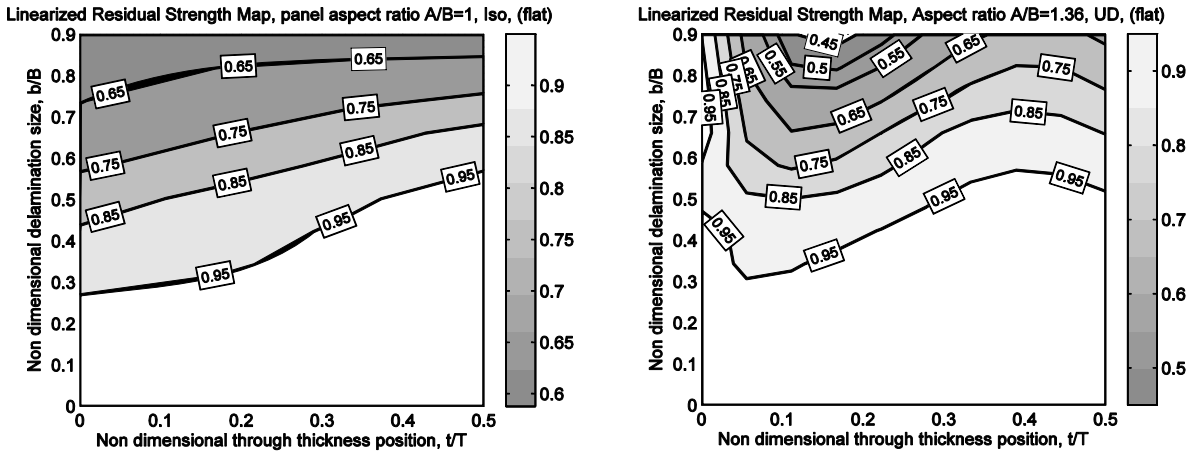

Figure 2.4 Reduced compressive strength for flat panels as a function of delamination size and through thickness position for isotropic material and unidirectional (UD) composite material respectively.

2.3.3 Compressive strength of curved panels

In this work slightly curved panels are analyzed. These are curved perpendicular to the loading direction with curvature height of 6% in comparison with the panel width.

The buckling mode maps illustrate the panel's response to uniaxial compression. These are made in a similar manner as was done by (Short et al. 2002). The maps can be divided into:

- Local buckling; seen for large delaminations close to the surface
- Global buckling; seen for small and deep delaminations

The buckling mode map for the slightly curved panels is found in Figure 2.5 and for the flat panels in (Sørensen et al. 2009).

A corresponding strength reduction map for the curved panels is shown in Figure 2.6.

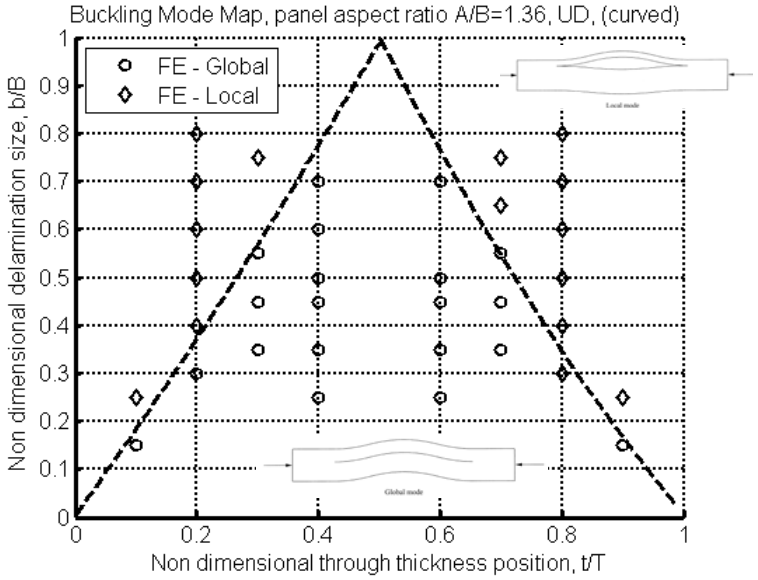

Figure 2.5 Buckling mode map for slightly curved panels. Buckling mode is shown as a function of delamination size and through thickness position for unidirectional (UD) composite material. t/T = 0 corresponds to the convex (outer) side of the panel.

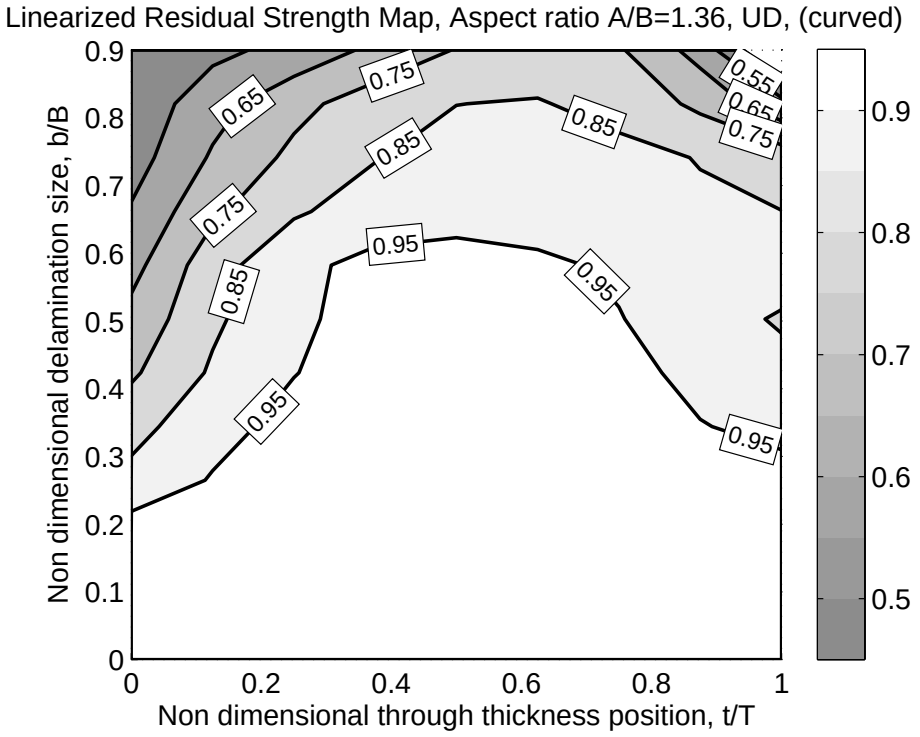

Figure 2.6 Reduced compressive strength for slightly curved panels as a function of delamination size and through thickness position for unidirectional (UD) composite material.

2.4 Discussion and conclusions

In Figure 2.7 is the buckling behavior shown for flat UD panels and compared with the experimental results for the panels tested in Phase 3 and Phase 4. It is found that there generally is a good agreement between the predicted buckling behavior and the observed behavior during the experiments. The numerical analyses give a quite sharp borderline between the local and global buckling modes. For the experiments this borderline cannot be expected to be sharp and the experiments also indicate that there is band along the borderline where both local and global buckling behavior can be expected. This band seems to be wider as the delaminations get bigger and deeper in the panels. This also agrees with the sub-mode area found for the numerical analyses. However more experiments and analyses are needed to obtain more solid conclusions on this band.

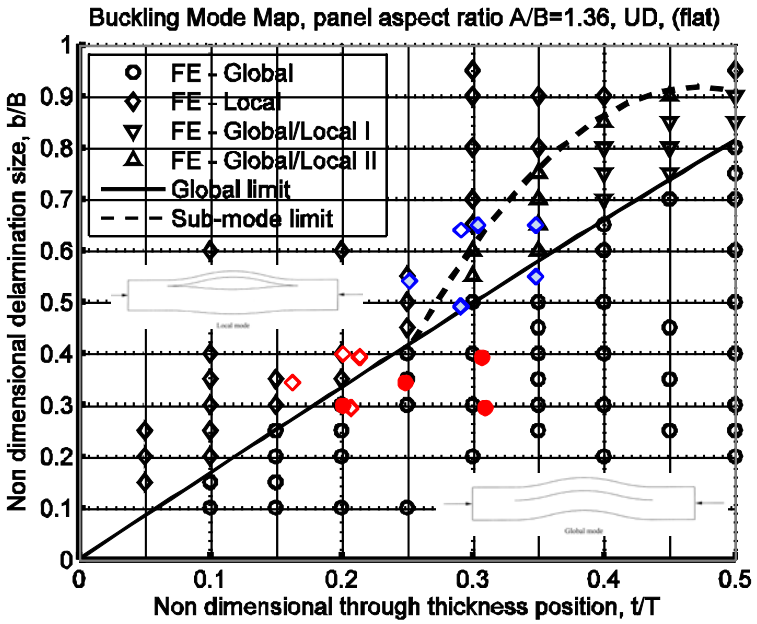

Figure 2.7 Buckling mode map for flat UD panels with experimental results included. Type A panels are red and type B panels blue. Solid circles mean global buckling while diamonds mean local buckling. The light blue colored diamonds mean that the local behavior is uncertain or the panel sometime shown global behavior.

The reduced compressive strength for flat UD panels is shown in Figure 2.8, where also the experimental data from Table 1 is included. It is generally found that the reduced compressive strength is larger for the experiments than predicted by the FE-analyses. This is particularly true for the B type panels, where the strength is reduced more due to delaminations than found for the A type panels. This may be due to the fact that bigger and deeper delaminations have larger strength reduction, but the manufacturing process for the B type panels may also result in higher sensitivity against delaminations than seen for the A type panels. More experiments and in-depth analyses are needed in order to make more solid conclusions on the higher observed strength reduction.

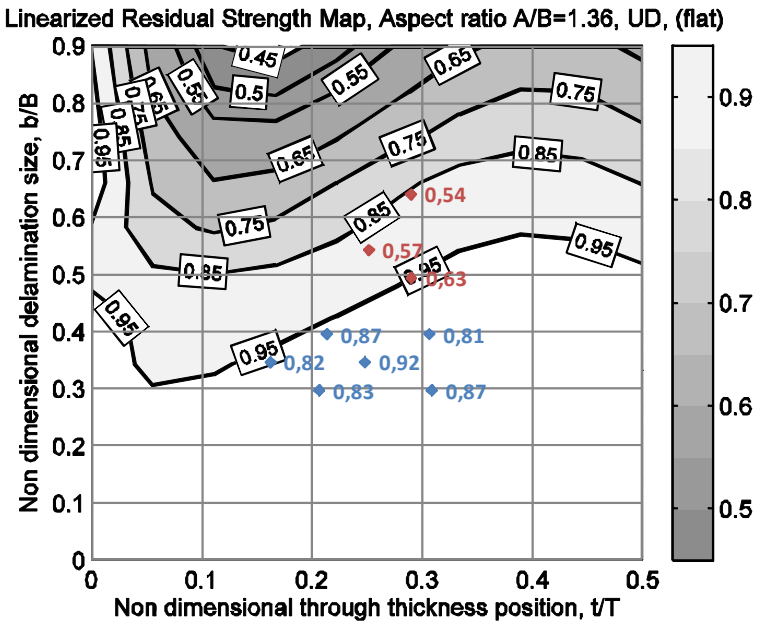

Figure 2.8 Reduced compressive strength for flat UD panels with experimental data included. Type A panels are red and type B panels blue. The labels indicate the average reduced buckling load factor from the experiments.

3 Materials joints

3.1 New approach for analysis of DCB laminate specimens

3.1.1 Background

Delamination (crack growth along weak interfaces between plies in composite laminates) is one of the most encountered failure modes in wind turbine blades (Sørensen et al., 2004). In order to design wind turbines safely, i.e. to avoid delamination growth, fracture mechanics methods are required for the characterisation for the fracture resistance of the interfaces, e.g. in terns of a fracture energy or a cohesive law. The common procedure involves testing a specimen with a well-defined crack, recording the load level at which the crack propagates, and calculating the potential energy release rate or the J integral using analytical solutions or - for more complicated laminates - numerical models based on classic laminate theory. This calculation is somewhat involving for laminates consisting of plies having orthotropic elastic properties, since the stacking sequence of the laminate must be known along with the thickness, the elastic properties and fibre orientation of each layer. It is therefore of interest to develop simpler approaches.

In the following, a new approach, based on measurement of curvature of beams, are described. The idea was studied in a Master project (Rask, 2009) conducted at SDU under the supervision of Jørgen B. Pedersen, SDU and B. F. Sørensen, Risø DTU. The Master project won the "Kompositsektionens F&U pris 2009".

3.1.2 The overall idea

The specimen in focus is a double cantilever beam specimen loaded with uneven bending moments (DCB-UBM) (Sørensen et al., 2006). A sketch of the specimen and applied loads are given in Fig. 3.1.

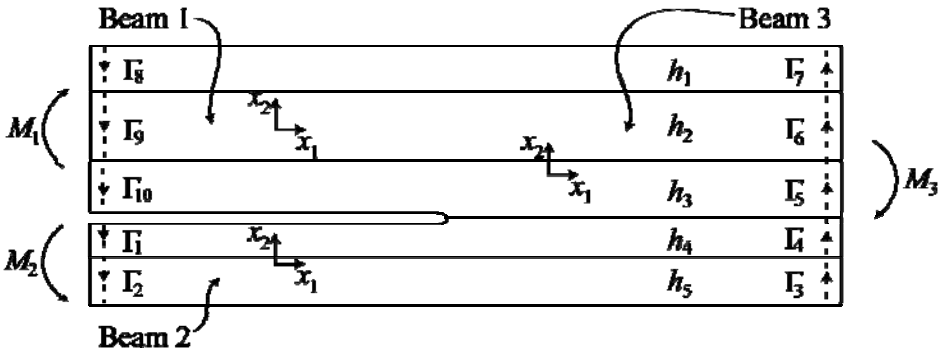

Figure 3.1 A laminate DCB specimen, consisting of five layers of different material types and/or orientations, are loaded with uneven bending moments (DCB-UBM). From (Rask, 2009).

A major assumption in the following is that all layers in the laminate behave linear-elastically (the same assumption is made in the analysis based on the laminate theory [CLL], so the following approach is not more restrictive). Then, when loaded with pure bending moments, the axial strain ε_{11} will vary linearly across the thickness of each beam. An application of the J integral of a beam-end gives - since the beam is subjected to pure bending -

$$J_i = \frac{\kappa_i^0 M_i}{2B} \tag{3.1}$$

where M_i is the bending moment applied to beam end number *i*, *B* is the width of the specimen and κ_i^0 is the curvature of the neutral axis of the beam, giving by

$$\kappa_i^0 = \frac{1}{R_i} \tag{3.2}$$

where R_i is the radius of curvature of the neutral axis of beam number *i*. The radius of curvature is taken positive when the beam bends downwards and negative when the beam bends upwards. The J integral evaluated around the external boundaries of the DCB-specimen simply becomes the sum of J integral evaluated across the three beam ends. It follows that Jext can be determined experimentally if the applied moments, M1 and M_2 as well as the curvatures of beam number 1, 2 and 3, denoted κ_1^0, κ_2^0 and κ_3^0, are measured. This approach is new. We call it *the curvature approach.*

3.1.3 Experimental validation

The proposed approach was validated experimentally by analysing fracture mechanics test by both the curvature approach and by a method based on laminate theory (Lundgaard-Larsen et al., 2008). The latter requires complete information regarding the thickness and elastic properties of each layer.

Specimens made from laminates consisting of 12 layers of two different types of laminas. The resulting beam thickness *H* was ≈ 10 mm and *B* ≈ 30 mm. Strain gauges were bonded to the beams to record the axial strains. The beams were bonded together using an adhesive layer to form a sandwich specimen. An insert and a slip foil were placed at the end of the adhesive layer to facilitate crack propagation along the

laminate/adhesive interface. Fig. 3.2 shows a part of a typical specimen; strain gauges can be seen.

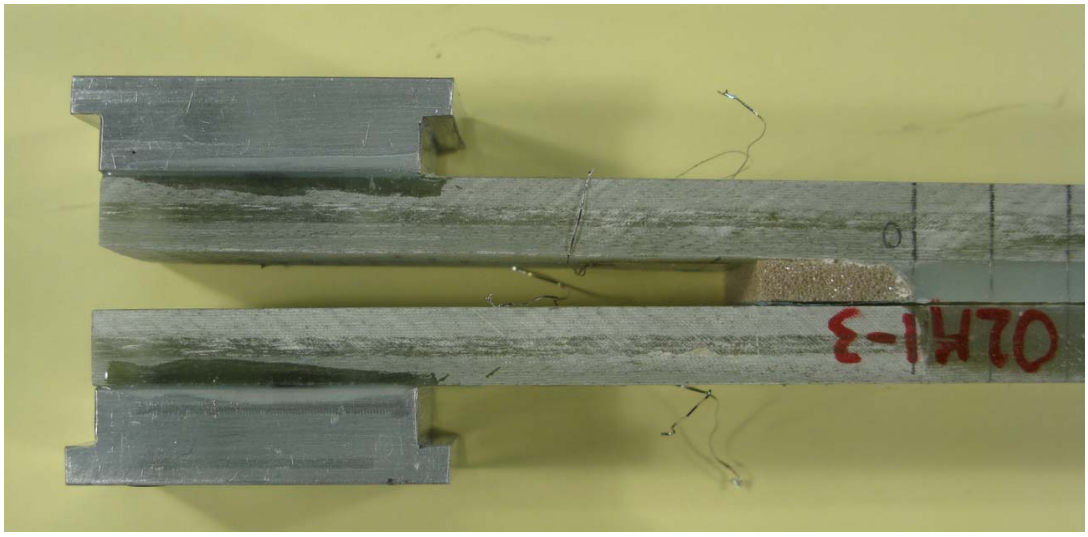

Figure 3.2 Cracked end of DCB specimens consisting of two laminates bonded together. The thickness of the beams is 9 mm. Steel parts for applying moments are bonded to the left-end of the specimen. The crack is situated between the adhesive layer and the lower beam (seen to the right hand side of image).

The curvature of each beam was obtained from the axial strain at the top and bottom of the beam:

$$\kappa_i^0 = \frac{\left(\varepsilon_{11}^+\right)_i - \left(\varepsilon_{11}^-\right)_i}{H}, \tag{3.3}$$

where $\left(\varepsilon_{11}^+\right)_i$ and $\left(\varepsilon_{11}^-\right)_i$ are the strains at the top and bottom of the beam and H is the beam thickness.

Fig. 3.3 shows a typical result of a fracture mechanics test. J calculated from the curvature approach and by the model based on laminate theory (Lundgaard-Larsen et al., 2008) follows each other reasonably close. Ideally, the two curves should lie on top of each other, since they represent two different ways of calculating the same value, the J integral. The differences can be attributed to uncertainties in the thicknesses and elastic properties of the layers used in the model based on laminate theory.

For the particular test shown in Fig. 3.3, the onset of crack growth is identified by a small drop in J (indicative of a small drop in J) give the fracture energy $J_c \approx$ 445-500 J/m^2. This value corresponds to the fracture energy, viz., the energy that is taken up by the crack tip, as it propagates along the adhesive/laminate interface. The subsequent crack propagation occurred fairly stable. The J integral values increases with increasing crack length (R-curve behaviour) due to fibre bridging, reaching a steady-state value J_{ss} of about 1500-2000 J/m^2.

Note that the curvature approach requires no knowledge about the thickness, ply orientation and elastic properties of the laminate, just the laminate thickness and width, H and B.

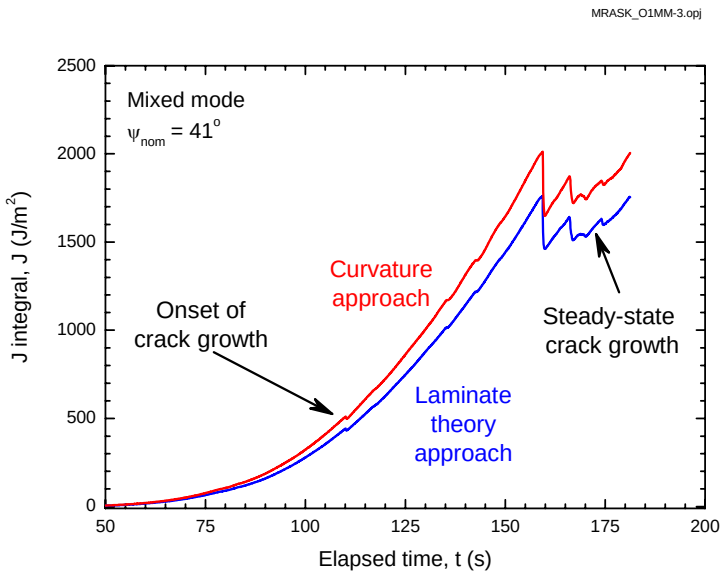

Figure 3.3 The J integral value, calculated from the curvature approach and a model based on laminate theory, is shown as a function of time. Arrow indicates the onset of cracking.

3.2 Simulation of fracture of medium size specimens

The aim here is to investigate if cohesive laws, determined from double cantilever beam specimens loaded with uneven bending moments (DCB-UBM) (Sørensen et al., 2006) can be used for predicting the load level for the propagation of an interface crack between two uneven composite materials in larger medium size specimens that have a different size, geometry and loading that the DCB specimens.

3.2.1 Geometry, finite element mesh and boundary conditions

The finite element method (Abaqus vs 6.8-2) was used to model the crack growth along the interface of the two different composite materials (laminates). In order to facilitate the analysis of the simulations symmetry conditions were assumed (see Fig. 3.4), thus only half of the medium size specimen was modelled. Only one thickness for the short beam was modelled (H = 10 mm). Both laminates were glass fibre composites. The boundary conditions prescribed were: $u_2 = 0$ at the symmetry plane ($x_2 = 0$), where u_i is the displacement vector (the subscript refers to the direction of the displacement, where x_i is the coordinate axis, see Fig. 3.4). At x_1 = 1200 mm, the edge was constrained in the x_1 direction ($u_1 = 0$). The external loading was applied in displacement control, u_1, at ($x_1 = 0$).

The crack growth at the interface of the two composite laminates was modelled using 4-noded cohesive elements. A finite cohesive element thickness (h_c = 0.005 mm) was used to avoid interpenetration of the two laminates. The selected thickness corresponds to 4% of the cohesive element length. The finite element mesh used near the cohesive zone is shown in Fig. 3.4b (at x_1 = 440 mm). It can be seen that for the composite laminates, four-node elements and three-node elements were used. This combination allows for efficient mesh transitions.

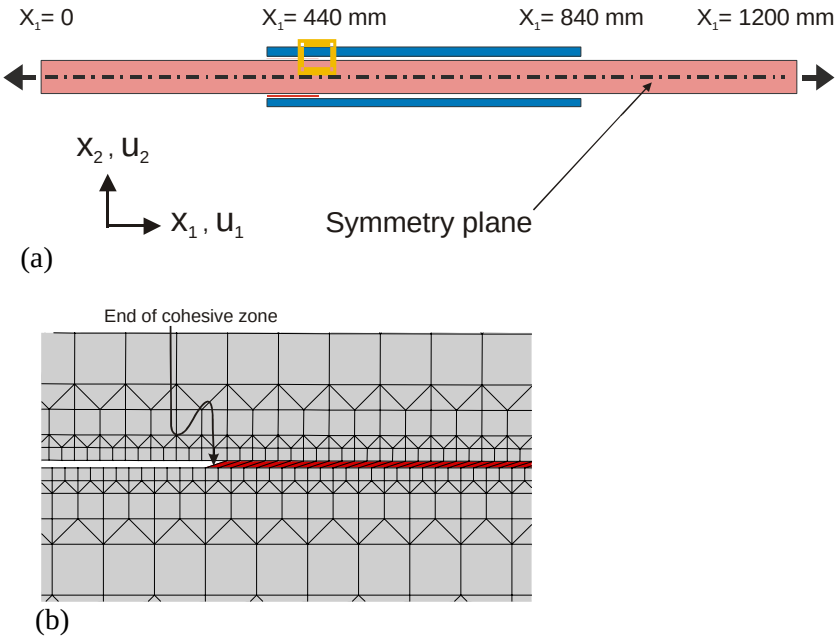

Figure 3.4 a) Geometry of the medium size specimen, and b) deformed finite element mesh near the end of cohesive zone. The cohesive elements are illustrated by red colour.

3.2.2 Material properties and cohesive law parameters

The composite laminates were modelled as isotropic, linear elastic solids with E_1 = 12.60 GPa for the middle laminate and E_2 = 11.86 GPa for the side laminates. For both materials, the Poisson's ratio was set equal to 0.3.

The cohesive law parameters were approximated from the DCB-UBM experiments described elsewhere (Sørensen et al., 2009). Two idealised cohesive laws were assumed for all mode mixities: linear and exponential softening. Three (not independent) parameters are needed for the complete description of the selected cohesive laws: steady-state fracture resistance, critical opening and peak stress. Since the steady state fracture energy, J_{ss}, and the critical opening are more accurately measured from the experiments, the peak stresses were adjusted so that area under the stress-separation curve equals J_{ss} for the measured critical openings for the specific mode mixity. Fig. 3.5 shows a typical DCB-UBM experiment where J_{ss} and the critical opening are shown (the specimens were made in the laboratory and their properties are therefore not representative of materials used in real wind turbines). As it can be seen from Fig. 3.5, it is not easy to pinpoint a clear steady-state situation, and the exact value of the steady-state fracture energy, J_{ss}, and the critical opening are somewhat arbitrary chosen.

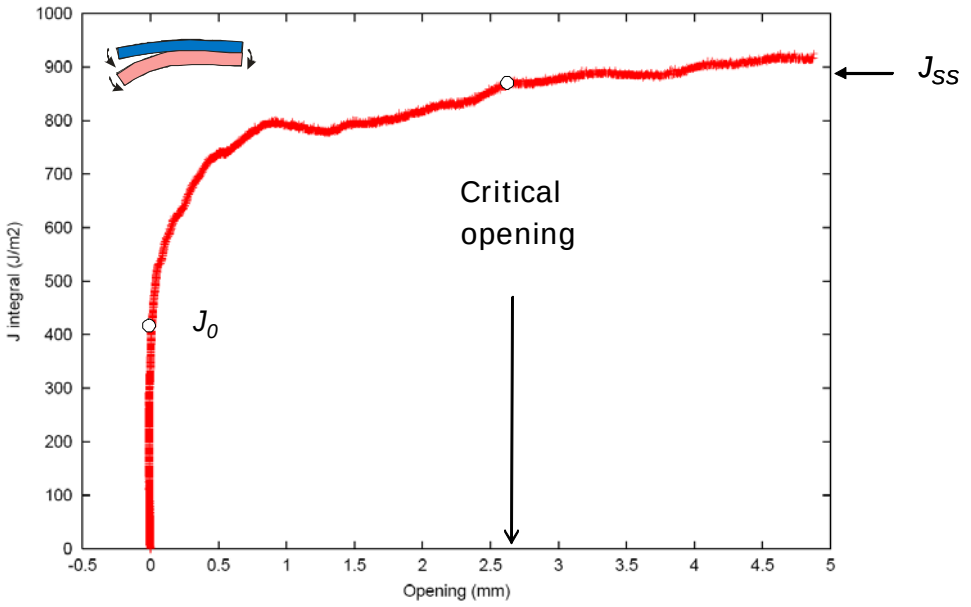

Figure 3.5 Measured fracture resistance, J_R, as a function of the end-opening. J_o is the initiation, and J_{ss} the steady-state fracture resistance.

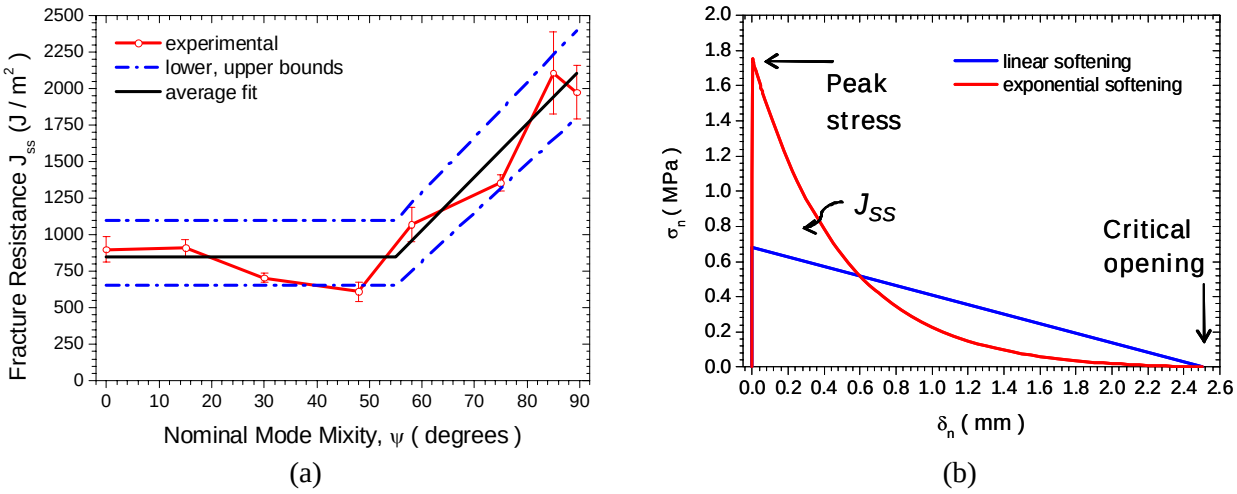

Figure 3.6 a) Measured steady-state fracture resistance as function of the nominal mode mixity and b) examples of linear and exponential softening laws for Mode I (the area under the curves equals J_{ss}).

Three different estimations (for simplicity bilinear functions) of the J_{ss} as a function of the phase angle were performed (it is assumed that the phase angle is the same as the nominal mode mixity): average fit and lower and upper bounds of the experimental data as can be seen in Fig. 3.6a. The peak stresses for Mode I and Mode II were calculated from the critical opening and the steady state fracture resistance for Mode I and II, respectively and the assumed softening law. Fig. 3.6b shows the Mode I cohesive laws for the linear and exponential cohesive laws. For mixed-mode conditions, the total

fracture resistance is taken from Fig. 3.7a and a quadratic traction failure criterion was used for damage initiation in the cohesive elements according to:

$$\left(\frac{\hat{\sigma}_n(\varphi)}{\hat{\sigma}_n}\right)^2+\left(\frac{\hat{\sigma}_t(\varphi)}{\hat{\sigma}_t}\right)^2=1 \tag{3.4}$$

where $\hat{\sigma}_n$ is the peak stress for pure Mode I and $\hat{\sigma}_t$ is the peak stress under pure Mode II.

3.2.3 Solution method

It is well-known that implicit solvers encounter convergence problems since the stiffness matrix becomes ill-conditioned as the crack grows and a steady state condition is approached. A number of numerical stabilisation techniques exist to overcome this problem but in general it is difficult to achieve steady-state conditions. Therefore, an explicit (dynamic) solver was used for the problem of Fig. 3.7 under quasi-static conditions. In all cases it was ensured that the kinetic and artificially dissipated energy was less than 1% of the strain energy to minimise the dynamic effects associated with the explicit solver.

3.2.4 Comparison of predictions and measurements

The numerical predictions for the load as a function of crack extension are given in Fig. 3.8 for the linear and exponential cohesive laws and the different estimations of the fracture resistance as a function of nominal mode mixity (see Fig. 3.6a). The experimental data from one specimen are also included. For the case of a linear softening law the experimental data lie between the estimated upper and lower bounds except for long crack extensions where the predicted loads are higher than the measured loads. For short cracks, the simulations based on the exponential softening laws over predict the loads determined experimentally, as the peak cohesive stress is much higher than in the case of linear softening (see Fig. 3.6b). For long cracks, the simulations based on exponential softening under predict the experimental results. Most likely the actual cohesive law lies in between the two idealised cohesive laws used here.

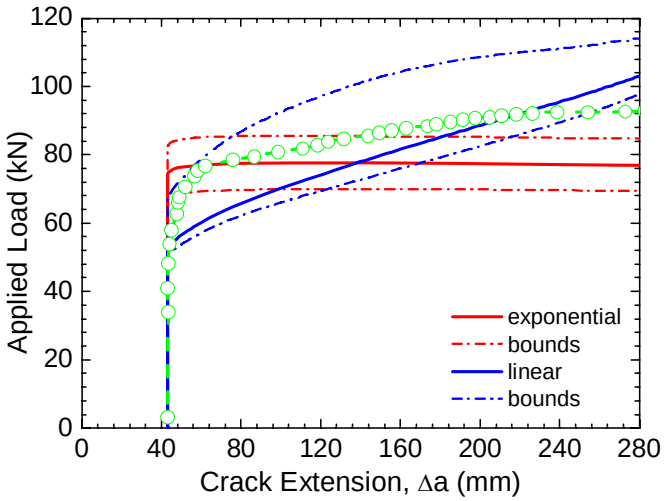

Figure 3.8 Predicted and measured (open circles) component behaviour. Red lines indicate an exponential softening law and lines in blue a linear softening law.

The use of mixed mode cohesive laws, obtained from DCB-UBM experiments, was demonstrated for strength prediction of medium scale specimens. The predictions were made using idealised linear or exponential softening cohesive laws. The next step is to use more precise non-linear cohesive laws and use a full model with two different cohesive laws for the two interfaces of the medium size specimens as during the experiments the crack at one of the interface usually propagates faster than the other one which suggests that the interface fracture resistance differs for the two interfaces of the specimen.

4 Cyclic crack growth with large-scale bridging

4.1 Motivation and purpose

Wind turbine blades will be subjected to varying wind loads during their expected 20-years service life. Thus, there is a risk that they can develop fatigue damage and fatigue crack growth (e.g. delamination in laminates, adhesive joints and sandwich panels). It is therefore of great importance to establish knowledge and methods that can be used for assessing how fast cracks grow due to cyclic loading.

Observations show that under monotonically increasing load, many composite materials develop large-scale bridging during cracking. From a structural safety point of view, the formation of a large-scale bridging zone is desirable, since it increases the fracture resistance (Sørensen and Jacobsen, 1998). It is of great interest to know if large-scale bridging also retards cyclic crack growth.

Furthermore, large-scale bridging complicates the analysis of specimens and the interpretation of experimental results. Standard linear-elastic fracture mechanics (LEFM) test methods are not applicable (Suo et al., 1992). Under large-scale bridging, fatigue crack growth involves cyclic crack growth at the main crack tip as well as the

degradation of the bridging ligaments behind the crack tip. The mechanical response of the large-scale bridging zone can be expressed in terms of a traction-separation law, denoted a bridging law; the bridging law experienced during cyclic loading is likely to differ from that operating under monotonic opening.

The purpose of this study is to develop an experimental test method for the characterising mixed mode crack growth under cyclic loading of composite materials exhibiting large-scale bridging.

4.2 Test method

Several issues are of importance in the development of the new test method. First, since the J integral (Rice, 1968) can be used for analysing large-scale bridging problems (Suo et al., 1992), it is preferable to use a specimen (geometry and loads) for which an analytical J integral solution (J evaluated along the external boundary) exist also for large-scale bridging. Second, it is preferable to study cyclic crack growth under constant conditions, so the effect of the bridging zone can be properly characterised. Thus, while the test method as such should be able to generate different mixed mode loadings (from Mode I to Mode II), the amount of Mode I and Mode II should remain the same throughout an experiment. Third, it is preferable if the test method can be implemented at a standard materials testing machine, so that the method can easily be implemented in the wind energy community.

The test specimen configuration proposed in the present study is the double cantilever beams specimen loaded with uneven bending moments (DCB-UBM). This method was developed in an earlier EFP-project (Sørensen et al., 2004) for monotonically increasing loading. This test specimen belongs to a small family of steady-state DCB specimens (loaded with axial forces and/or bending moments) for which the J integral can be obtained in close analytical form (Suo et al., 1992) - the solutions for J are valid for (and independent of) the properties of the large-scale bridging zone. The J integral gives a rigorously correct connection between the crack tip stress field, the bridging zone and the J integral evaluated along the external boundaries.

4.3 Practical implementation

The developed test method was designed to be mounted at a standard materials testing machine (Instron 88R 1332). Some of the design ideas and principles of the existing static loading device (Sørensen et al., 2004) are used: The uncracked end of the specimen is fixed at a central support; transverse arms are mounted at the two beams at the other end of the specimen. The uneven pure bending moments are created by different distances between rollers (different moment arms) of forces of equal magnitude but opposite direction applied to transverse arms by a wire. The wire runs from an upper beam, where two load cells are mounted, to the transverse arms, down to a lower beam via rollers, past a servo-hydraulic actuator and up again on the other side. In order to minimize errors in the applied moments as a result of specimen deflection, the distance between the transverse arms and the upper and lower rollers is maximised by mounting the load cells on a transverse beam above the upper cross-member, giving long wire lengths (See Fig. 4.1). The cyclic load is generated by the servo-hydraulic actuator that is mounted upside down on the materials testing machine, see Fig. 4.1 and Fig. 4.2.

4.4 Identification of allowable test window

After the manufacturing and assembling the hardware parts, the first step was to verify that the test method could perform as intended. One worry was that the long wires might induce unwanted vibrations, that might cause the actual moment applied to the DCB-UBM specimen to differ from that intended (e.g. distorting the load-as-a-function-of-time and creating out-of phase loadings at the arms of the DCB specimen). Therefore, a comprehensive test programme was undertaken (Rasmussen, 2010) in order to establish practical limits to load levels, loading frequency, mode mixity, etc. As a part of the testing program, a DCB-specimen reinforced with 8 mm steel skin was equipped with strain gauges at each cracked beam. Data from the two load cells, the strain gauges and an extensometer were recorded and analysed.

The major results from this investigation can be summarised as follows: A loading frequency of 2-3 Hz seems to work fine for all transverse arm lengths. Higher loading frequencies may be possible under Mode I (symmetric loading) than for Mode II. Furthermore, higher loading frequencies are possible for the transverse arms having short lengths. The length of the crack does not have a significant effect. Fig. 4.3 shows an example of recorded data, shown as a function of time for loading situation corresponding to near Mode II. Ideally, all recorded data should vary in a sinusoidal fashion as a function of time. This is well obtained for the 2 Hz experiment, but for a loading frequency of 6 Hz, the signal from the extensometer (recording the opening of the beams) shows a significant (undesirable) distortion.

4.5 Initial test results

The first tests were made on specimens made of a unidirectional glass fibre polymer matrix composite - i.e., providing data for characterisation of cyclic growth of delamination cracks. The specimens were cut from a plate manufactured in the laboratory by vacuum infusion. A slip foil had been inserted to act as a starter crack.

A 10 Mpixel digital camera (Canon D200) was mounted at the test machine, so that the crack length could be recorded after specific number of load cycles. A special control set-up was used for controlling both the servo-hydraulic actuator and the camera. The cyclic load varied in a sinusoidal shape between fixed maximum and minimum loads at 2 Hz, i.e., between fixed maximum and minimum moments (and thus constant maximum and minimum values of J). The crack length was determined from the images.

Generally, the crack length was found to increases fastest in the early stages, i.e. when the crack was short. With increasing crack extension, the crack growth rate decreased significantly, particularly for Mode I tests. Fig. 4.4 shows some typical results. It is seen from Fig. 4.4 that the crack growth rate decreases as a function of time, eventually reaching a constant rate. Note also that there is only a small difference between the crack extension of the three specimens tested under identical conditions.

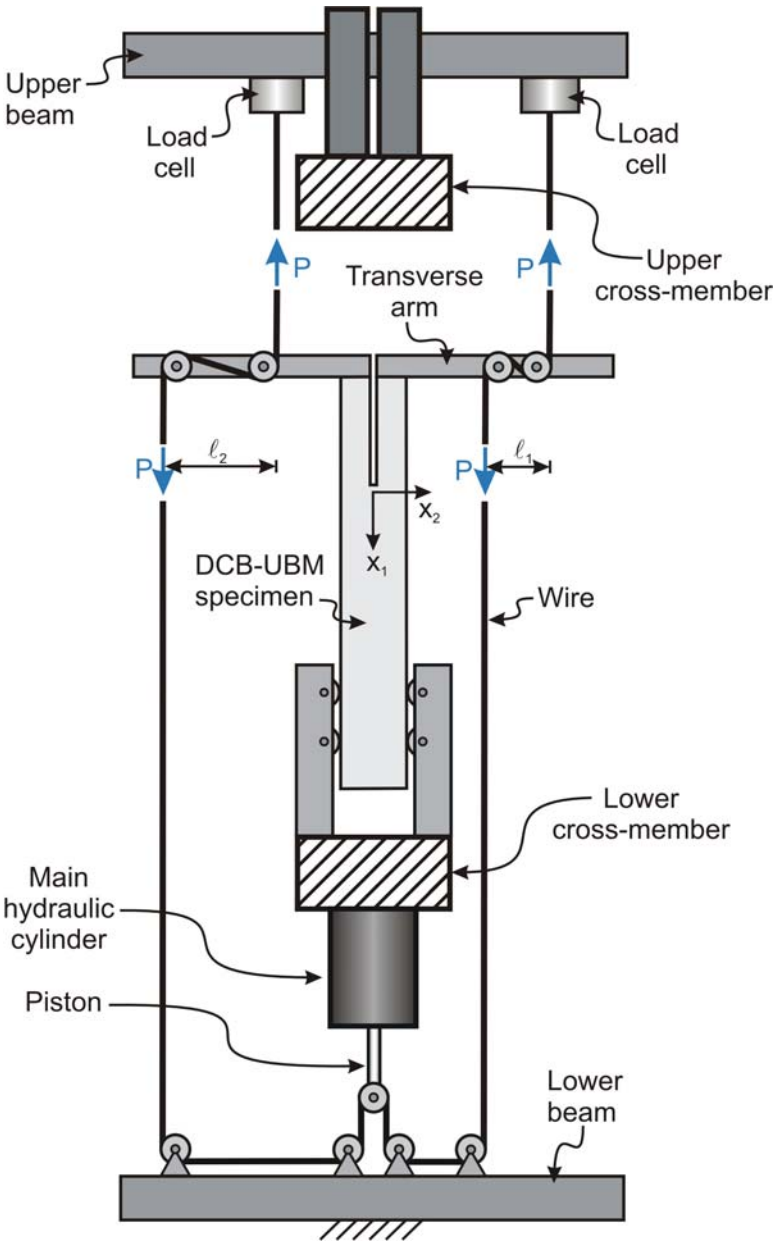

Figure 4.1 Sketch of the cyclic loading device.

Figure 4.2 Photo of the developed cyclic loading device.

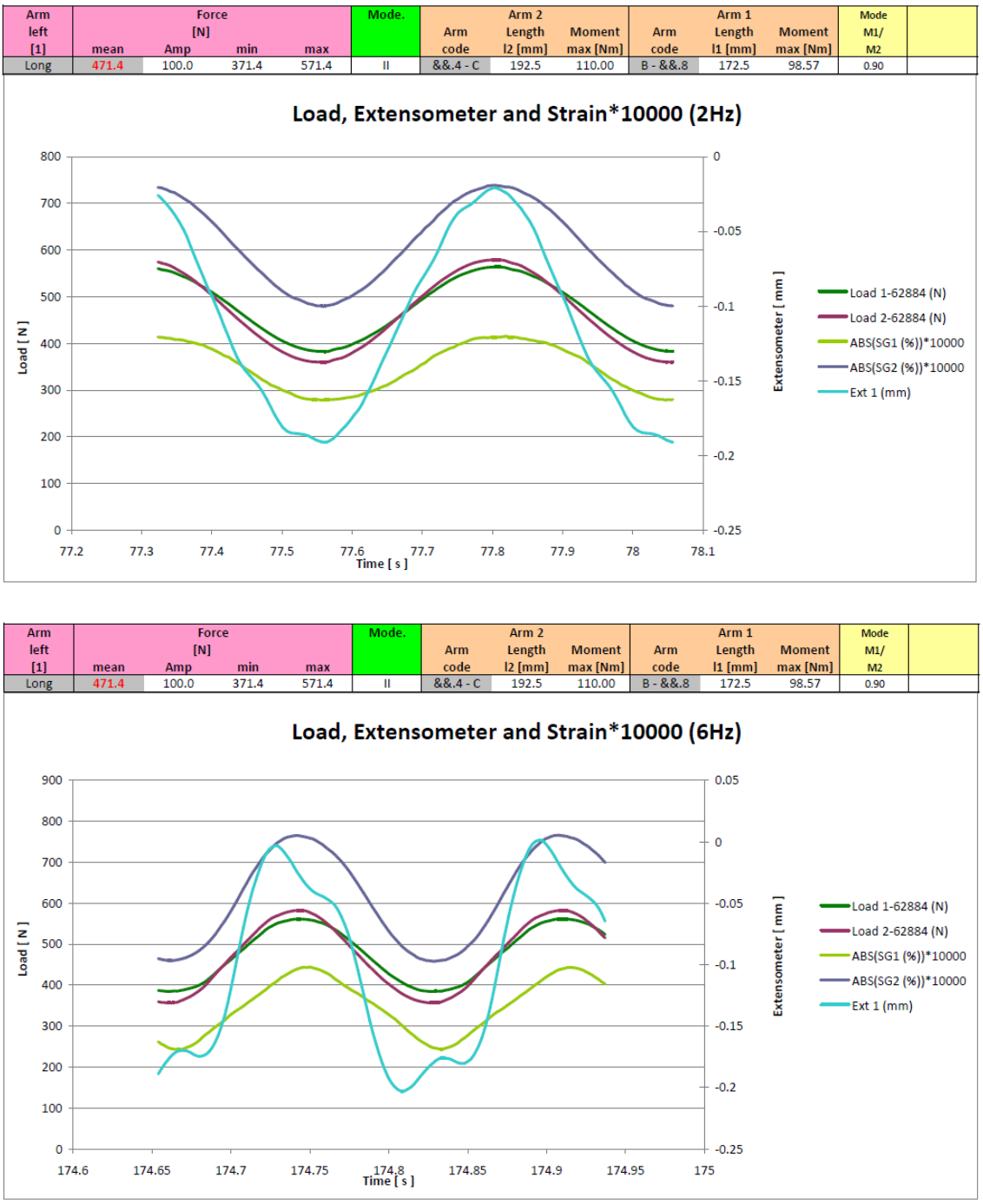

Figure 4.3 Example of recorded data (loads from two load cells, strains at arms of DCB-specimen and crack opening as a function of time for two loading frequencies (2Hz and 6 Hz) for a near full Mode II loading with the longest transverse arms.

The results can be understood as follows. Initially, in the very early stages of cycling, the crack is virtually without bridging. Thus, the growth rate in the early stages represents the crack growth rate on a near-unbridged crack. With increasing number of cycles, the crack tip advances away from the initial starter crack (the slip foil), creating a bridging zone between the end of the slip foil and the crack tip. Within the bridging zone, ligaments of unbroken fibres and single fibres transmit stresses between the crack faces,

effectively unloading the crack tip stress field. The decrease in the crack tip stress field reduces the growth rate of the crack tip. With increasing number of cycles, the bridging zone length increases. However, bridging ligaments may also fail in the bridging zone. Eventually all ligaments have failed at the location of the crack starter, creating a finite-length (fully developed) bridging zone. Then, a steady-state situation can be anticipated: The crack tip and the bridging zone translate along the specimens in a self-similar fashion, creating a constant growth rate. It is concluded, that from an engineering point of view, the presence of a large-scale bridging zone is beneficial under cyclic loading, since it slow down the growth of delamination cracks significantly.

The perspective is that the steady-state crack growth rate can be used for prediction the cracks in large wind turbine structures. The steady-state crack growth under a fully-developed large-scale bridging zone also provides information regarding the degradation of the bridging ligaments under cyclic loading. As such, it may provide useful information for the development of future interfaces that are more resistant to cyclic crack growth.

Finally, the fact that a steady-state crack growth rate is obtained using the DCB-UBM specimen shows the usefulness of this specimen configuration for the study of cyclic crack growth in materials experiencing large scale-bridging. Other test specimens would not allow the fully-developed bridging zone to retain a constant length and thus generating the steady-state, constant growth rate.

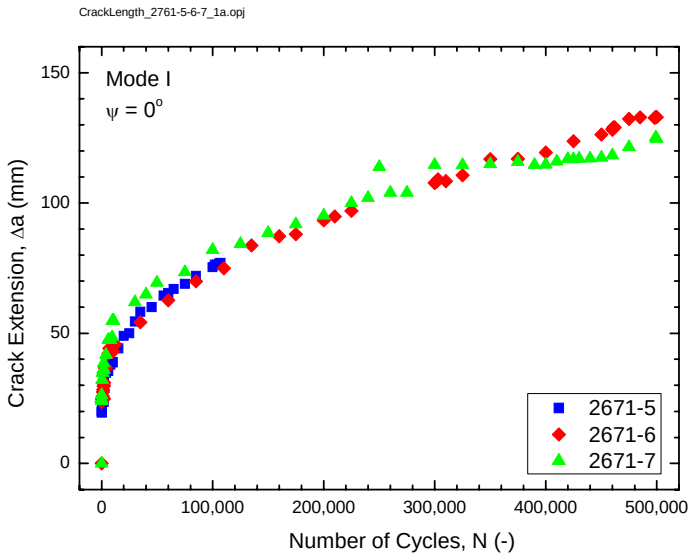

Figure 4.4 The crack extension is shown as a function of the number of load cycles for 3 specimens cycled under identical, constant conditions (i.e., fixed Jmax and Jmin).

4.6 Future work

With the test method established and demonstrated, there are now possibilities for conducted a number of crack growth studies, which can form the basis for the formulation of phenomenological crack growth laws. Effects that should be studied includes effects of mode mixity, effect of the mean J value, load-history effects (e.g. effects of few high load cycles on subsequent low load cyclic crack growth), loading frequency, humidity, temperature, etc.

Future studies could also be directed towards the development of micromechanical model that includes fatigue crack growth of the main crack tip as well as cyclic degradation of the bridging ligaments.

It is also possible to transfer the developed testing approach to wind turbine industries that have their own materials testing machines.

5 Modelling of blade with damage

5.1 Static analysis of sections of wind turbine blade involving geometric and material instabilities

Numerical simulations of laminated structures consume significant CPU resources due to the necessity to treat each of the lamina separately and this is especially true when treating structures as complex as wind turbine blades. In order to reduce the necessary CPU resources for completing an analysis, the effort has concentrated on two areas. First the inhouse developed FE-code MUST utilized for the numerical simulations has been *parallelized* (MPI and OpenMP) on all compute intensive tasks including the computation and assembly of residuals, jacobian matrices, and linear/nonlinear solvers. The effort allows efficient utilization of more simultaneous cores and multiple compute nodes on the supercomputer “Fyrkat”, thereby significantly reducing the wall clock time required to complete the numerical analysis. Secondly, effort has been expended on improving and *tuning the element routines* used in analysis of laminated structures, such that computations on each element are performed faster, thus improving the overall efficiency.

The combined effect of the above code improvements/optimizations makes it possible to analyze larger and more realistic problems and models, or alternatively to execute the numerical analysis in a fraction of the time on the developed models in Phase 3 regarding static analysis of wing sections with geometric and material instabilities.

5.2 Simulation of crack growth under cyclic loading

Initial preparations for enabling fatigue and crack problems to be performed within the finite element code MUST has focused on finding simple constitutive models for estimation of crack growth rate and propagation in order to be able to use tabulated material parameters available from established literature. Besides material parameters, the crack growth rate and direction depend on the stress and strain state at the crack tip. The state is established by knowing the current loading of the structure and current geometry, taking into account any geometric nonlinearities present in the analysis, and taking into account any degradation of the crack interface that has already occurred and is causing a change of the geometry of the cracked wind turbine blade. This includes stiffness degradations and newly formed cracks caused by delamination/fatigue growth of past events.

Quasi static analysis is used to estimate crack growth rate and rate of damage in the current situation, and subsequently a new configuration is established by the used of explicit integration of the rates. Code reuse is substantial from the established models from Phase 3, including most book-keeping of damage parameters. Being able to land at a specific load level for use in the integration of the crack is important for the estimation of the growth rates, and to this end an improved arc-length solver has been developed that also takes into account specifications about delamination and crack growth

parameters in the control criteria. Computed rates are quite sensitive to the actual loads applied, and thus the ability to be able to land on specific load levels is quite important in contrast to a quasi static progressive delamination analysis where degradation over time (load cycles) is not taken into account.

The actual integration formulas for the crack growth rates should be based on adaptively selecting step sizes for the crack growth such that the accuracy of the simulation can be maintained at a sufficient level throughout. No such scheme has been implemented due to numerical problems encountered with the cohesive model/elements used that had to be resolved before more progress could be made.

It was the intention that several constitutive models should have been tested to evaluate their predictive capabilities but the initial studies revealed several problems with the implementation of the cohesive elements. The implementation used in MUST is based on the same methodology as the one used in the commercial finite element code ABACUS. For the cohesive elements, a standard bilinear constitutive relation is used. The problem is related to the behavior of the constitutive law for the cohesive elements and the numerical integration used within each element. To better illustrate the problem, consider the generic example shown in Fig. 5.1.

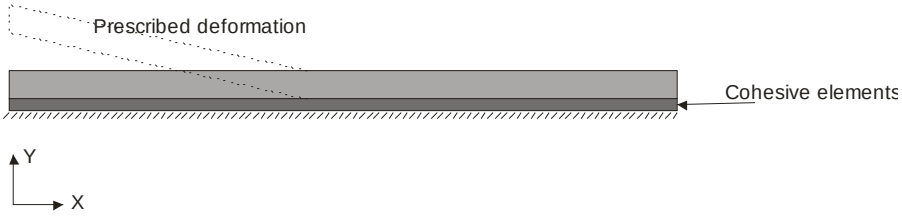

Figure 5.1 A test example with prescribed displacements of cohesive elements.

In the test example, the displacement (and thereby crack opening) in the y-direction is given as $v(x, y, t) = k \max(0, t - x)$, where k is a constant chosen in relation to the dimensions of the test example, and t is a pseudo time. Note that with this displacement field imposed, the form of the cohesive zone is constant for all t after the cohesive zone has fully developed, and therefore the resulting force in the cohesive elements should be constant.

The response predicted for the cohesive force with very small steps on the pseudo time and using a coarse discretization and a finer discretization is shown in Fig. 5.2.

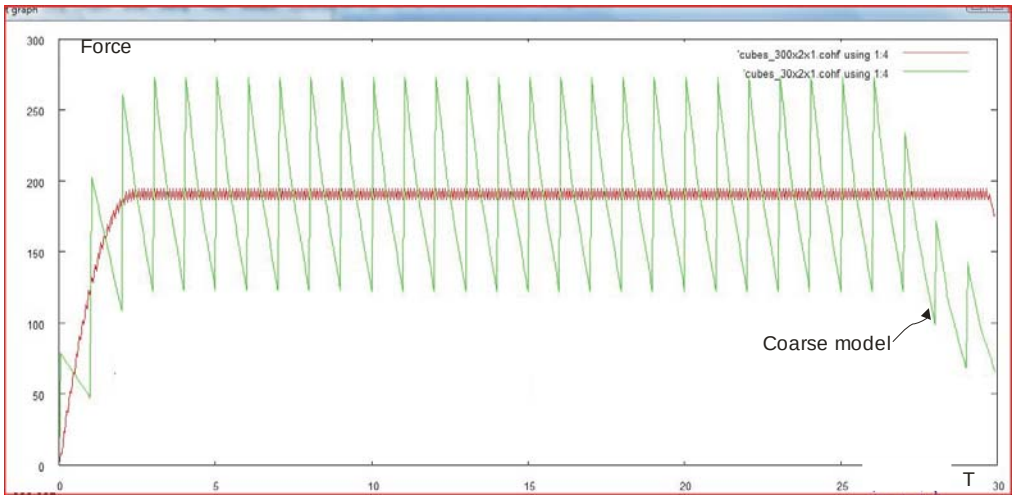

Figure 5.2 Predicted load as a function of time for two simulations using different meshes, a coarse mesh (green colour) and a fine mesh (red color).

The large oscillations in the resultant force have been found to be a result of the numerical integration of the constitutive law used within the elements, and not a result of the constitutive law itself. As such, using a smoothed constitutive law will not remove the oscillations, but merely smooth the response curve a bit. The problem with using a model like this for prediction of fatigue and crack propagation is that extreme mesh sensitivity of the results is to be expected, as well as making the control of the numerical solution accuracy very challenging. Note also, that the fine discretization displays the same oscillations albeit on a smaller scale, and the numerical problems with controlling accuracy would likely persist to some extent through mesh refinement.

A solution to partly remove the oscillatory behavior has been found by modifying the numerical integration within each of the cohesive elements. Consider the two situations A and B in Fig. 5.3, where a bilinear constitutive relation is used for the cohesive elements and three elements are used in the cohesive zone.

In both situations the integration points used in a standard two-point numerical integration of the cohesive force is indicated by a gray dot. It can be reasoned that for both situations the element to the left will give an inaccurate prediction of the resultant of the cohesive tractions. Moreover the resultant will spike every time an integration point passes the maximum traction supported by the interface. Situation A corresponds to the negative slope on the response graph, and vice versa. Typically, this has been alleviated by using mesh refinement in the cohesive zone. A rule of thumb has been to use 10 elements in the zone, but as the typical extent of the cohesive zone of a carbon fibre/epoxy is about 3-4mm this becomes prohibitive in large scale analysis.

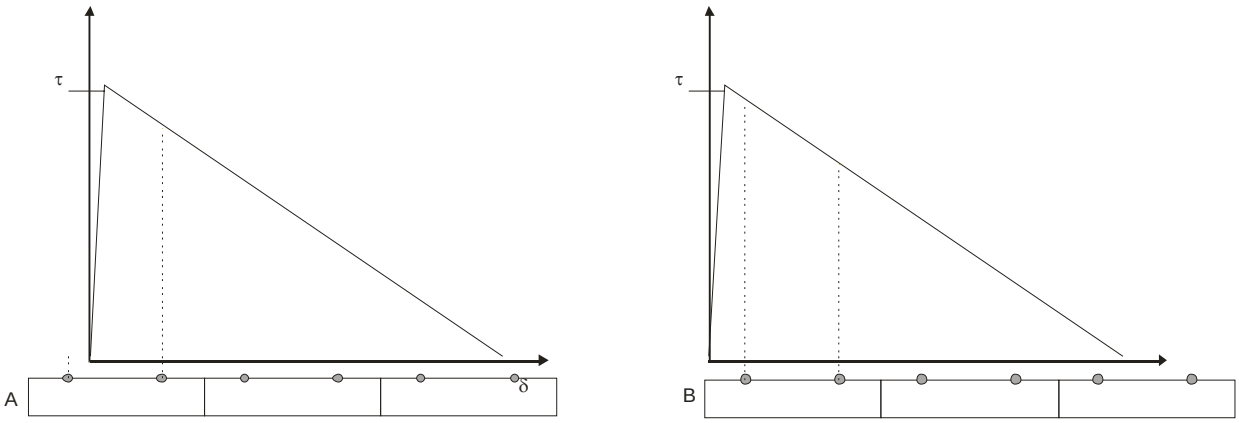

Figure 5.3 The cohesive stresses in points for numerical integration depend strongly on the exact position of the points within the cohesive zone in a coarse mesh.

In MUST an improved numerical quadrature based on composite Newton Cotes has been implemented and studies have shown that the improved accuracy in the integration of the constitutive law alleviates the jagged response to a large extent. The number of integration points used inside each element is set to a “high” number (typically several hundred in 3D), and this is of course unsatisfactory from a performance point of view for general application. Several further improvements are possible. One would be to adaptively select the number of quadrature points inside each element when using a composite rule, and another would be to subdivide the element integration into regions with a simple behavior in each region. None of the improvements has been implemented, because the percentage of time spent in the cohesive elements is low compared to the overall analysis time.

As a bonus the improved integration has made the actual solution of the nonlinear overall problem much easier, i.e. convergence is achieved in significantly less iterations, resulting in a much reduced solution time for the FE-models despite the increased time spent on integration of the cohesive elements. At present the improved integration utilized in the cohesive elements is not available in commercial programs.

Due to the unexpected problems with the oscillatory behavior of the cohesive interface, time has not allowed a working implementation for simulation of crack growth during fatigue to be reached. It was deemed necessary to first obtain a code that was able to provide accurate solutions for each step used for the simulation of the propagation, and as such the result of the work done in Phase 4 has been more concentrated on further improvements of the work performed under Phase 3 to actually allow for the use of the methods in the prediction of crack growth under fatigue.

6 Discussion and conclusions

6.1 Implementation in Industry: LM Wind Power A/S

The theory developed in the project is used extensively at LM and fracture mechanics is now a key competence in the company. The area has been strongly reinforced during the last few years both by developing the competencies of the employees and by hiring. The knowledge developed through the EUDP project is used as reference to the internal work done in the fracture mechanics area in the company.

The test method used to assess the cohesive interface law is impelemented in the company alongside with the methods of calculating the J-integral for any layup.

The principles of hirachical modelling developed through the EUDP project and implemented in the FE-system MUST at Aalborg University are followed closely and investigations of the principles behind the method are looked into. This in order to improve the correlation between blade test results and FE results in the future.

The stability tests carried through with the compressive tests of composite panels with delaminations have been followed and may be used to setting up criteria for allowable delaminations in blades.

6.2 Implementation in the industry: Vestas Wind Systems A/S

The work in the project has been followed closely in Vestas. The project has developed important reference cases for description of damage progress in laminates in testing and in analytical models. Vestas uses the project as a starting point for implementing advanced models for dealing with defects and damage in design, manuacturing, testing and operation and maintenance.

The laboratory test methods developed in the project are relevant for measuring the material parameters that control damage growth.

6.3 Summary

The major result in the area of compressive strength of flat composite panels with delaminations is:

- A good agreement was found between buckling behaviour (global versus local buckling) measured experimentally and predictions based on numerical simulations

The majors result within the area of fracture mechanical characterisation of materials joints between dissimilar materials are:

- A new, simplified approach for the determination of the J integral for laminated DCB-UBM specimens was developed theoretically and validated experimentally against an approach based on laminate theory; a good agreement was found for the two approaches
- The propagation of a crack along an interface between two dissimilar composite materials was simulated by the use of idealised mixed mode cohesive laws (the cohesive law parameters were obtained from independent DCB-UBM

experiments); a good agreement was found between model predictions and experimental results

The major results in the area of cyclic crack growth with large-scale bridging are:

- A testing equipment was developed for applying cyclic, pure uneven bending moments for a DCB-specimen (DCB-UBM); the loading device is mounted at a standard materials testing machine
- Under cyclic crack growth, a steady-state situation developed for a material exhibiting large-scale bridging: a steady-state crack growth rate, much lower than the crack growth rate of an unbridged crack, was obtained.

The major result concerning the implementation of advanced cohesive laws is:

- An improved numerical quadrature-based on Newton Cotes, implemented in the finite element code MUST, showed an improved accuracy in the integration of the cohesive law

A number of scientific publications have emerged from the project. A list of 6 journal papers, 14 conference papers, one contribution to a book and two reports are listed in Section 7.

6.4 Suggestions for future work

The results obtained in this research project (Phase 4) suggest further research in coming research projects. Examples are:

- Modelling of buckling-driven delamination of curved composite panels
- Modelling of interface cracking in bimaterial specimens using mixed mode cohesive laws that are more realistic than the idealised ones used so far
- The work on cyclic crack growth involving large scale bridging of this study represents only a very first step. Much more should be done in future research projects, e.g. study crack growth rate under various environmental conditions, effects of loading sequence, changes in applied mode mixity etc. The studies should lead to materials laws for the cyclic degradation of the bridging zone. They can be purely phenomenological or micromechanically based
- Study the development of damage from processing flaws to cracks (where fracture mechanics can be applied)

7 Publications from current project

7.1 Journal publications

Brøndsted, P., Holmes, J. W, and Sørensen, B. F., 2008, "Wind turbine rotor blade materials technology", *European Sustainable Energy Review*, Vol. 2, pp. 36-41.

Hansen, A. L. and Lund, E., 2009, ”A Mixed mode cohesive law for modeling interfacial fracture and fiber bridging”, *Int. Journal of Solids and Structures*, under review, 26 pp.

Hansen, A. L., Sørensen, B. F., and Lund, E., 2009,”Simulation of crack growth and R-curve behavior using cohesive zone modeling”, manuscript in progress, 16 pp.

Holmes, J. W., Rasmussen, U. R. and Sørensen, B. F., 2010, "Experimental technique for mixed-mode cyclic crack growth testing of composite laminates". *Engineering Fracture Mechanics*, manuscript in preparation.

Quispitupa, A., Berggreen, C., and Sørensen, B. F., 2010, "Parametric determination of the mode-mixity for debonded sandwich specimens under mixed mode bending", manuscript in preparation.

Toft, H. S., Branner, K., Berring, P. and Sørensen, J. D., "Defect distribution and reliability assessment of wind turbine blades", *Engineering Structures* (submitted).

7.2 Conference proceedings

Berggreen, C., Tsouvalis, N., Hayman, B. & Branner, K., "Buckling strength of thick composite panels in wind turbine blades – Part I: Effect of geometrical imperfections", in Proc. 4th International Conference on Composites Testing and Model Identification, 20-22 October 2008, Dayton, Ohio, USA.

Branner, K., Berring, P. & Berggreen, C., "Buckling strength of thick composite panels in wind turbine blades – part II: Effect of delamination", in Proc. 4th International Conference on Composites Testing and Model Identification, 20-22 October 2008, Dayton, Ohio, USA.

Branner, K., Bitsche, R.D. & Jensen, F.M., , 2010, "Effect of strain rate on sandwich web failure in the load carrying girder of a wind turbine blade", in: Proc. of 9th International Conference on Sandwich Structures, 14-16 June 2010, California Institute of Technology, Pasadena, California, USA.

Hansen, A.L., Lund, E., Pinho, S.T., Robinson, P. and Branner, K., 2009, "A hierarchical FEM approach for simulation of geometrical and material induced instability of composite structures", in: Proc. of Composites 2009, 2nd ECCOMAS Thematic Conference on the Mechanical Response of Composites, 1-3 April 2009, Imperial College, London, UK.

Luczak M., Branner K., Kahsin M., Martyniuk K., Peeters B. and Ostachowicz W., 2010, "Applying static and dynamic test responses for defect prediction in wind turbine blades using a probabilistic approach", in: Proc. of European Wind Energy Conference and Exhibition (EWEC), 20-23 April 2010, Warsaw, Poland.

Luczak M., Peeters B., Mevel L., Döhler M., Ostachowicz W., Malinowski P., Wandowski, T. and Branner K., 2010, "Damage detection in wind turbine blade panels using three different SHM techniques", in: Proc. of IMAC XXVIII, 1-4 February 2010 Florida, USA.

Luczak M., Peeters B., Szkudlarek W., Mevel L., Döhler M., Ostachowicz W., Branner K. and Martyniuk K., 2009, "Comparison of the three different approaches for damage detection in the part of the composite wind turbine blade", in: Proc. of IWSHM 2009, 9-11 September 2009, Stanford, CA, USA.

Lund, E., and Møller, H. (2009): "Eigenvalue sensitivity analysis and optimization in structural design problems". In: Proc. 22nd Nordic Seminar on Computational Mechanics, NSCM22 (eds. L. Damkilde, L.A. Andersen, A.S. Kristensen and E. Lund), 21-23 October, 2009, Aalborg, Denmark, Department of Civil Engineering, Aalborg University, DCE Technical Memorandum, No. 11, ISSN 1901-7278, pp. 345 - 354.

Moslemian, R., Berggreen, C., Branner, K. and Carlsson, L. A., 2008, "On the effect of curvature in debonded sandwich panels subjected to compressive loading", in Proc. 8th International Conference on Sandwich Structures, 6-8 May 2008, University of Porto, Portugal.

Paik, J.K., Branner, K., Choo, Y.S., Czujko, J., Fujikubo, M., Gordo, J.M., Parmentier, G., Iaccarino, R., O'Neil, S., Pasqualino, I., Wang, D., Wang, X. and Zhang, S., "Ultimate strength", Committee III.1, in: Proc. of 17th International Ship and Offshore Structures Congress, ISSC'2009, 16-21 August 2009, Seoul, Korea.

Szkudlarek W., Kahsin M., Luczak M., Peeters B., Kurowski M., Branner K., Martyniuk K., Wasilczuk M., 2009, "Vibration-based damage detection in multilayer composite material", in: Proc. of ICSV16, 5-9 July 2009, Krakow, Poland.

Sørensen, B. F., 2009, "Materials and structures for wind turbine rotor blades - an overview", in Proc. ICCM-17, 17th International Conference on Composite Materials, 27 Jul 2009 - 31 Jul 2009, Edinburgh International Convention Centre (EICC), Edinburgh, UK.

Toft, H. S., Branner, K., Berring, P., Bode, J., Wedel-Heinen, J. & Sørensen, J. D., 2009, "Distribution of defects in wind turbine blades", in: Proc. of European Wind Energy Conference and Exhibition (EWEC), 16-19 March 2009, Marseille, France.

Toftegaard, H., Goutianos, S., and Sørensen, B. F., 2009, "Interfacial crack growth in bimaterial composite specimens", in Proc. ICCM-17, 17th International Conference on Composite Materials, 27 Jul 2009 - 31 Jul 2009, Edinburgh International Convention Centre (EICC), Edinburgh, UK.

7.3 Book contributions

Sørensen, B. F., Holmes, J. W., Brøndsted, P., and Branner, K., 2010, "Blade materials, testing methods and structural design", Chapter 13 in Wind Power Generation and Wind Turbine Design (edited by Dr. Wei Tong), WIT Press, pp.417-65.

7.4 Reports

Rask, M., 2009, "Crack development in composite materials", Master Thesis, Institute of Physics and Chemistry, University of Southern Denmark, Odense, Denmark.

Rasmussen, U. R., 2010, "Indledende undersøgelse for ny udmattelsestest", Risø-R-1735(DA), ISBN 978-87-550-3826-4, in progress.

8 Other publications

Abrate, S., 1991, "Impact on laminated composite materials", *Applied Mechanical Review*, Vol. 44, pp.155-190.

Lundsgaard-Larsen, C., Sørensen, B. F., Berggreen, C., and Østergaard, R. C., 2008, "A modified DCB sandwich specimen for measuring mixed-mode cohesive laws", *Engineering Fracture Mechanics*, Vol. 75, pp. 2514-30.

Short G. J., Guild F. J. , and Pavier, M. J., 2002. "Delaminations in flat and curved composite laminates subjected to compressive load", *Composite Structures*, Vol. 58, pp. 249–258.

Sørensen, B. F. and Jacobsen, T. K., 1998, "Large scale bridging in composites: R-curve and bridging laws", *Composites part A*, vol. 29A, pp. 1443-51.

Sørensen, B. F., Branner, K., Lund, E., Wedel-Heinen, J., and Garm, J. H., 2009, "Improved design of large wind turbine blades of fibre composites (Phase 3) - Summary Report". Risø-R-1699(EN), Risø DTU, Denmark.

Sørensen, B. F., Jørgensen, E., Debel, C. P., Jensen, F. M., Jensen, H. M., Jacobsen, T. K., and Halling, K., 2004, "Improved design of large wind turbine blade of fibre composites based on studies of scale effects (Phase 1). Summary report". Riso-R-1390(EN), Risø National Laboratory, Denmark.

Sørensen, B. F., Jørgensen, K., Jacobsen, T. K., and Østergaard, R. C., 2006, "DCB-specimen loaded with uneven bending moments", *International Journal of Fracture*, Vol. 141, pp. 159-172.

Suo, Z., Bao, G., Fan, B., and Wang, T. C., 1991, "Orthotropy rescaling and implications for fracture in composites", *Int. J. Solids Structures*, Vol. 28, pp. 235-48.

Risø DTU is the National Laboratory for Sustainable Energy. Our research focuses on development of energy technologies and systems with minimal effect on climate, and contributes to innovation, education and policy. Risø has large experimental facilities and interdisciplinary research environments, and includes the national centre for nuclear technologies.

Risø DTU
National Laboratory for Sustainable Energy
Technical University of Denmark

Frederiksborgvej 399
PO Box 49
DK-4000 Roskilde
Denmark
Phone +45 4677 4677
Fax +45 4677 5688

www.risoe.dtu.dk